Title:

SUMOylation of rice DELLA SLR1 modulates transcriptional responses and improves yield under salt stress

Authors:

Nuno M. Gonçalves[a*], Telma Fernandes[a], Cátia Nunes[b**], Margarida T. G. Rosa[a], Cleverson C. Matiolli[a], Mafalda A. A. Rodrigues[a], Pedro M. Barros[a], M. Margarida Oliveira[a], Isabel A. Abreu[a1]

Affiliations:

[a] Instituto de Tecnologia Química e Biológica, Universidade Nova de Lisboa (ITQB NOVA), 2780-157, Oeiras, Portugal

[b] Instituto de Biologia Experimental Tecnológica (iBET), 2780-157, Oeiras, Portugal

Author Contributions:

NMG participated in the conception of research, executed most experiments, and wrote the article with contributions from all authors. TF did protein interaction experiments. MTGR characterized SUMO-protease rice lines. CCM analysed data and completed the writing. MAAR purified recombinant proteins. PMB analysed RNA seq. MMO supervised experiments and analysed results. IAA conceived original project, supervised experiments, and finalised the article.

Contact:

[1] Corresponding Author:

Isabel A. Abreu

Instituto de Tecnologia Química e Biológica, Universidade Nova de Lisboa (ITQB NOVA), 2780-157, Oeiras, Portugal, Tel.: +351 214469647, E-mail: abreu@itqb.unl.pt

***** Currently at Leibniz Institute of Plant Biochemistry (IPB), Weinberg 3 | 06120 Halle | Germany (nunomiguel.goncalves@ipb-halle.de)

** Currently at Instituto Nacional de Investigação Agrária e Veterinária, Avenida da República, Oeiras, Portugal (catia.soares@iniav.pt)

Short title (50 characters): SUMOylation of rice SLR1 increases salt tolerance

ABSTRACT

DELLA proteins modulate GA signalling and are major regulators of plant plasticity to endure stress. DELLAs are mostly regulated at the post-translational level, and their activity relies on the interaction with upstream regulators and transcription factors (TFs). SUMOylation is a post-translational modification (PTM) capable of changing protein interaction and found to influence DELLA activity in Arabidopsis. We determined that SUMOylation of the single rice DELLA SLENDER RICE1 (SLR1) occurs in a lysine residue different from the one identified in Arabidopsis REPRESSOR OF GA (RGA), which suggests differential DELLA regulation by SUMOylation in monocots and dicots. Remarkably, artificially increasing SUMOylated SLR1 (SUMO1SLR1) levels attenuated the penalty of salt stress on plant yield. Gene expression analysis revealed that the overexpression of SUMOylated SLR1 regulates key dioxygenases that modulate active GA levels, namely *GA20ox2* and *GA2ox3*, which could partially explain the sustained productivity upon salt stress imposition. Besides, SLR1 SUMOylation blocked the interaction with the growth regulator YAB4, which may fine-tune *GA20ox2* expression. Mechanistically, we propose that SLR1 SUMOylation disrupts the interaction with members of several transcription factor families to modulate gene expression. We found that SLR1 SUMOylation represents a novel mechanism modulating DELLA activity, which attenuates the impact of stress on plant performance.

Keywords: DELLA, SUMOylation, stress, productivity, SLR1, YAB4, BZIP23, gibberellin

One sentence summary: Rice plants show increased yield under salt stress when its gibberellin transcriptional regulator DELLA protein is artificially SUMOylated.

INTRODUCTION

Salinity is one of the most serious threats to food security, affecting 20% of irrigated soils worldwide. Rice (*Oryza sativa* L.) is a crop with high sensitivity to salinity compared to other monocot crops, such as wheat and barley (Munns and Tester, 2008). Plant sessile nature requires rapid physiological responses to cope with stress, which is partly achieved through a complex crosstalk between hormone signalling pathways affecting growth, flowering, and defence against environmental challenges (Vanstraelen and Benková, 2012). Gibberellins (GA) are diterpenoid hormones involved in the regulation of several developmental processes, including seed germination, stem elongation, and flowering (Hirano et al., 2008). GA responses are modulated by DELLA proteins, which act as transcriptional regulators (Hedden and Thomas, 2012). In the presence of GA, DELLAs are targeted to ubiquitin-mediated proteasome degradation by the GA-receptor GA-INSENSITIVE DWARF1 (GID1) through binding to specific DELLA domains (DELLA/TVHYNP), followed by DELLA polyubiquitination mediated by the E3-ligase GA-INSENSITIVE DWARF2/SLEEPY1 (GID2/SLY1). When GA levels decrease, DELLA proteins accumulate and interact with key transcriptional regulators to restrain growth (Hirano et al., 2010; 2008; Ueguchi-Tanaka et al., 2008). For instance, DELLAs can sequester the transcription factors PHYTOCHROME INTERACTING FACTOR3 and 4 (PIF3 and PIF4), in addition to negatively regulate PIF3 protein abundance, mediating the crosstalk of light and GA signalling to modulate cell growth (de Lucas et al., 2008; Li et al., 2016). DELLA transcriptional regulation of GA biosynthetic genes responsible for hormonal homeostasis also potentiates growth arrest. The single rice DELLA SLENDER RICE1 (SLR1) interacts with YAB4 transcription factor to prevent the induction of *GA20ox2*, which encodes a dioxygenase that is essential for the synthesis of bioactive GA (Yang et al., 2016). In Arabidopsis, DELLA interaction with GAI-ASSOCIATED FACTOR1 (GAF1) TF triggers a negative-feedback loop that activates GA biosynthesis and subsequent DELLA degradation (Fukazawa et al., 2017). The increasing number of validated DELLA interactors showcase an overlap with most hormone pathways, impacting development, fertility, and seed number (Davière and Achard, 2015; Van De Velde et al., 2017).

DELLA activity is mostly modulated through post-translational modifications (PTMs), which impact its ability to interact with transcriptional regulators and modulate gene expression (Van De Velde et al., 2017). Besides ubiquitination and

97 subsequent proteasome-mediated degradation, there are other PTMs that influence
98 the activity of the DELLA's in response to GA signalling. For instance, the
99 phosphorylation by kinase EARLY FLOWERING 1 (EL1) regulates SLR1 protein
100 stability and activity (Dai and Xue, 2010; Itoh et al., 2005). Recently, a mechanism of
101 antagonistic PTMs was proposed to regulate Arabidopsis DELLA's interaction with
102 specific protein partners. *O*-fucosylation by SPINDLY (SPY) promotes DELLA
103 interaction with essential growth regulators – such as BRASSINOLE-RESISTANT1
104 (BZR1), PIF3 and PIF4 – leading to growth arrest (Zentella et al., 2017). Conversely,
105 SLR1 *O*-GlcNAcylation by SECRET AGENT (SEC) blocks these interactions and
106 promotes GA-induced growth resumption (Camut et al., 2017; Zentella et al., 2016).
107 DELLA SUMOylation has also been indicated as a PTM controlling the stability of
108 REPRESSOR OF GA (RGA), one of the Arabidopsis five DELLA proteins. SUMO
109 attachment to RGA hinders its ubiquitin-mediated proteasome degradation through
110 blockage of GID1-RGA interaction in a GA-independent manner (Conti et al., 2014).
111 The stabilization of Arabidopsis DELLA by SUMOylation also positively affected salt
112 stress response, in line with observations that DELLA accumulation leads to
113 increased salinity tolerance (Achard et al., 2006; Conti et al., 2014; Nelis et al.,
114 2015). SUMOylation is a eukaryotic ubiquitination-like process that involves the
115 processing, activation, conjugation, and ligation of mature SMALL UBIQUITIN-LIKE
116 MODIFIER (SUMO) to acceptor lysines (K) in the target protein (Miura et al., 2007).
117 Unlike ubiquitination, SUMO-modifications often occur in a canonical consensus
118 motif (ψ-<u>K</u>-X-E/D), which can be used for *in silico* prediction of SUMOylation targets
119 (Xue et al., 2006). SUMOylation regulates protein stability, activity, and interactions
120 with specific protein partners (Cremona et al., 2012). SUMO deconjugation
121 (deSUMOylation) from target proteins is performed by deSUMOylating proteases
122 (DSPs), with some members recently reported to be specific for poly-SUMO chain
123 processing (Eckhoff and Dohmen, 2015; Yates et al., 2016; Augustine et al., 2018).
124 In rice, reduced levels of SUMO conjugates due to DSP activity of OVERTOLERANT
125 TO SALT1/2 (OTS1/OTS2) have been connected to increased salt tolerance
126 (Srivastava et al., 2016a; 2016b). SUMOylation of specific TFs, such as the stress-
127 induced BASIC LEUCINE ZIPPER 23 (BZIP23), was suggested to be crucial to
128 drought tolerance and fertility (Srivastava et al., 2017).

Few studies have addressed the biological function of SUMOylation of stress-induced targets. Moreover, most of the studies investigating the effects of PTMs on DELLA function were done in Arabidopsis. This dicot model plant encodes five DELLAs in the genome and essentially differs from monocots, which harbour a single DELLA gene. This study demonstrates that SUMOylation of the single rice DELLA SLR1 impacts the transcriptional output in response to salt stress, possibly through modulation of SLR1 interaction with transcription factors regulating transcriptional patterns governing plant growth and stress responses. We suggest that SLR1 SUMOylation affects its interaction with key transcription factors that impacts GA homeostasis (YAB4), ABA signalling (BZIP23), and JA signalling (bHLH089/94). Additionally, the evidence provided suggests that it is possible to uncouple stress response from decreased plant performance by manipulating the levels of SUMOylated SLR1.

144 **RESULTS**

145 **SLR1 SUMOylation *in vitro* analysis suggests diversification of DELLA**
146 **regulation by SUMO in plants**

147 SUMOylation of lysine 65 (K65) in Arabidopsis DELLA RGA modulates its
148 stability in a GA-independent manner (Conti et al., 2014). To determine rice SLR1
149 SUMOylation, we started by performing an *in silico* prediction of SUMOylation motifs
150 using SUMOsp2 software (Xue et al., 2006) in rice DELLA SLR1 and Arabidopsis
151 DELLA RGA protein sequences. We sought for putative conserved SUMOylation
152 motifs in both proteins and found a low probability SUMOylation site which
153 corresponds to Arabidopsis RGA (Figure 1A). The SUMO acceptor lysine (K65) in
154 RGA is part of a canonical SUMOylation motif (LKLE). In contrast, its counterpart in
155 SLR1(K60) is not part of a canonical motif (QKLE), nor are the equivalent ones in
156 another Arabidopsis or monocot DELLAs (Supplemental Figure S1). Nevertheless,
157 both SLR1 and RGA have a high probability SUMOylation site on lysine 2 (K2).

158 To verify if the *in silico* prediction of SUMO attachment to SLR1 holds true, we
159 performed an *in vitro* SUMOylation assay targeting both full-length SLR1 and a
160 truncated isoform containing the leading 190 amino acids (SLR1t). Importantly,
161 SLR1t includes the N-terminal domains (DELLA and TVHYNP) responsible for GA-
162 mediated modulation of DELLA stability and SLR1 transactivation properties
163 (Davière and Achard, 2015; Marín-de la Rosa et al., 2015; Hirano et al., 2012), as
164 well as the predicted SUMOylation sites depicted in the Figure 1A. We observed a
165 mobility-shift of both full-length SLR1 (Figure 1B) and truncated SLR1t (Figure 1C;
166 with both SUMO1 and SUMO2 - Supplemental Figure S2A-B), consistent with ATP-
167 dependent SUMO-conjugation in the presence of the rice SUMOylation machinery.
168 The band resulting from *in vitro* SLR1 and SLR1t SUMOylation disappeared upon
169 treatment with recombinant SUMO-specific protease ULP1 that cleaves SUMO from
170 its conjugates (Li and Hochstrasser, 2003), confirming that the observed mobility-
171 shift was caused by attached SUMO (Figure 1B-C). To analyse the contribution of
172 each predicted SUMO acceptor lysine in SLR1, we performed directed mutagenesis
173 changing the lysines K2 and K60 to arginine residues, which cannot be conjugated
174 to SUMO (K2R and K60R). The mutated SLR1t K60R isoform retained the ability to
175 be SUMOylated – which was confirmed by the band disappearance after SUMO
176 proteolytic removal by ULP1 treatment – while K2R did not (Figure 1C). The result
177 shows that K2 is the preferential SUMOylated residue in SLR1, suggesting that

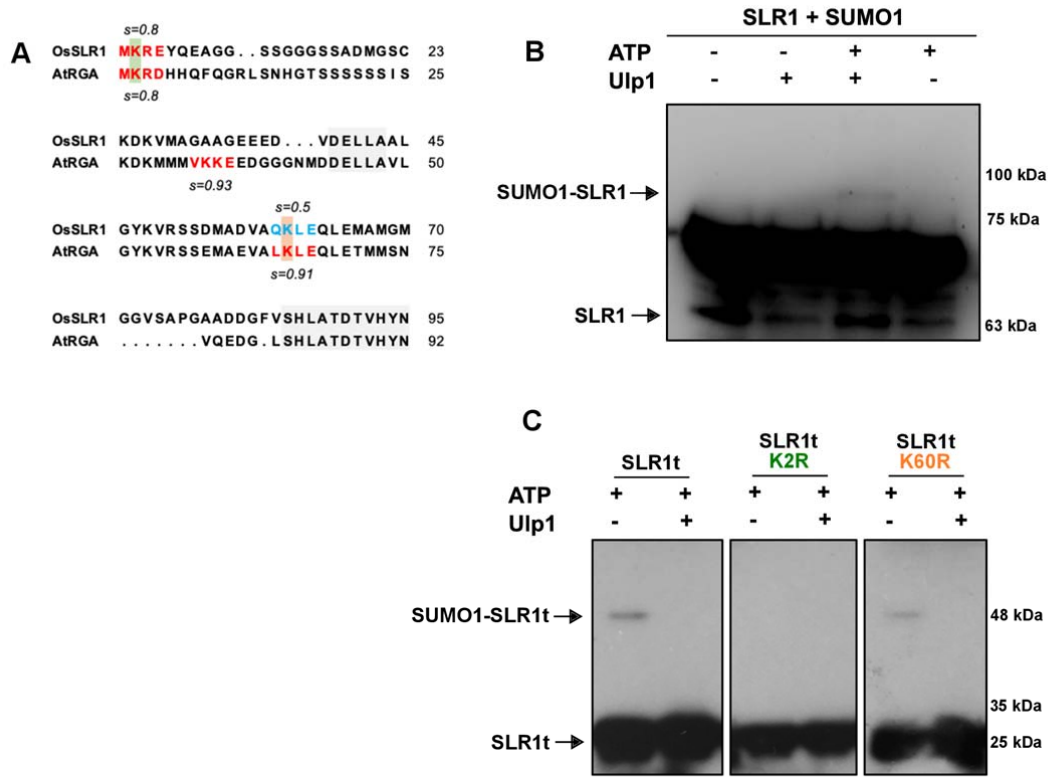

Figure 1. SLR1 is SUMOylated *in vitro* in a novel SUMO-conjugation canonical motif. **(A)** *in silico* prediction of SLR1 canonical motifs (ψ-K-X-E) in the N-terminal region as scored by SUMOsp2 software (Xue et al., 2006), compared to *Arabidopsis thaliana* RGA corresponding region. Motifs showing high SUMOylation probability are marked in red, and low probability motifs are marked in blue. SLR1 K2 and K60 are shown in green and orange, respectively. **(B-C)** *in vitro* SUMOylation assays using rice SUMOylation machinery (OsSCE1, OsSAE1/2, and OsSUMO1 = ~ 11 kDa) with recombinant SLR1 (~ 65 kDa) and SLR1t (~ 19 kDa) proteins, treated with ULP1 SUMO protease, as indicated. SLR1 and SLR1t were detected by immunoblotting using custom made anti-SLR1 antibody, where **(B)** corresponds to the full-length SLR1, and **(C)** to the SLR1 N-terminal truncated (SLR1t) coding the leading 190 first SLR1 residues, as well as the mutated isoforms SLR1t K2R and SLR1t K60R.

178 SUMO attachment to DELLA occurs in distinct lysine residues of Arabidopsis RGA
179 (K65) and rice SLR1 (K2). SUMOylation in different sites potentially results in
180 different outcomes regarding protein interactions and activity of SUMOylated SLR1
181 compared to SUMOylated RGA.
182
183 **SUMO protease activity analyses provide evidence of *in vivo* SLR1**
184 **SUMOylation**
185 To demonstrate the *in vivo* SUMOylation of SLR1, we treated non-denatured
186 rice protein extracts with the ULP1 SUMO protease. The procedure would allow for

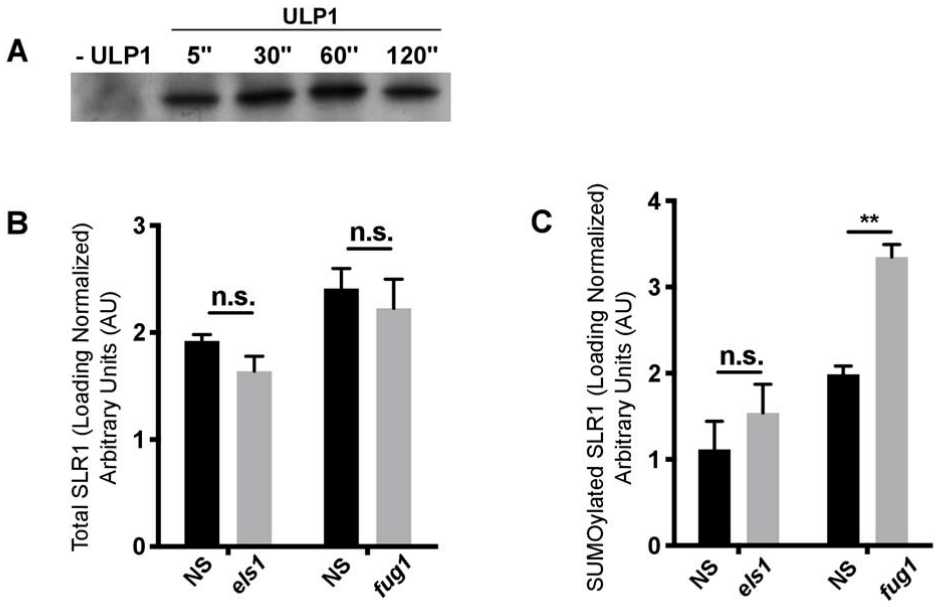

Figure 2. SUMO-specific protease activity reveal SLR1 *in vivo* regulation by SUMO. (A) *Oryza sativa* L. cv Nipponbare non-denaturing protein extracts treated with *Saccharomyces cerevisiae* Ulp1 (ULP1) for SLR1 deSUMOylation analysis as detected by immunoblot using anti-SLR1 antibody. **(B)** Loading-normalized relative quantification of total SLR1 protein in *els1* and *fug1* mutants, and the respective negative segregants (NS) after deSUMOylation by ULP1 treatment**;** and **(C)** total SUMOylated SLR1, as shown by ratio comparison to non-SUMOylated protein after ULP1 treatment. Error bars correspond to standard error (SE; n=4). Statistically significant values are represented as **($p<0.01$).

187 indirect detection of SUMOylated SLR1 by analysing the increase in non-
188 SUMOylated SLR1 protein amount resulting from ULP1 treatment, in comparison to
189 SUMOylated SLR1. We observed an increase of non-SUMOylated SLR1 upon the
190 addition of ULP1, as detected by the anti-SLR1 antibody in protein extracts (Figure
191 2A). The result is in line with the previous *in silico* and *in vitro* analyses indicating
192 that SLR1 could be SUMOylated. Our results also suggest that SLR1 mono-
193 SUMOylation may be much less abundant than other forms of SUMOylation since
194 we could not detect an SLR1 band with the expected mobility shift for mono-
195 SUMOylation (Figure 1B-C). To further support the evidence of *in vivo* SLR1
196 SUMOylation, we tested the levels of SUMOylated SLR1 in knockout mutant lines for
197 genes encoding rice SUMO proteases, namely *els1* and *fug1* (Figure 2B-C). ELS1
198 and FUG1 are active rice SUMO proteases, as both knockout lines contain
199 increased levels of SUMOylated proteins (Rosa et al., 2018). We treated protein
200 extracts from *els1* and *fug1* homozygous lines with ULP1 and compared their total

201 SUMOylated SLR1 levels with those present in negative segregant lines (NS). The
202 results show that although the overall level of non-SUMOylated SLR1 is not
203 significantly affected in either one of the KO lines when compared to their negative
204 segregant lines (Figure 2B), the levels of SUMOylated SLR1 are increased in *fug1*
205 mutant (Figure 2C). These results demonstrate SUMOylation of SLR1 occurs *in vivo*,
206 as indicated by the processing (*i.e.,* switch from SUMO-SLR1 to SLR1) mediated by
207 FUG1. Interestingly, it also suggests that there is a certain degree of specificity for
208 SLR1 deSUMOylation, as suggested by SUMO cleavage by FUG1 and not ELS1
209 (Figure 2C). Altogether, the evidence supports that SLR1 is SUMOylated *in planta*
210 and that SUMO specific proteases could regulate the levels of SUMOylated SLR1.
211

212 **Overexpression of SUMOylated SLR1 increases salt tolerance**

213 Because DELLA protein accumulation was previously connected with stress
214 tolerance (Achard et al., 2006), we assessed SLR1 expression in response to salt
215 stress. Wild-type seedlings accumulated SLR1 protein in shoots during the first 8
216 hours of stress (Supplemental Figure S3A). On the other hand, *SLR1* transcript
217 levels decreased, which is consistent with the previously reported DELLA negative
218 feedback-loop regulation on its own transcript abundance (Hedden & Thomas,
219 2012).

220 To gain insight on the role of SLR1 SUMOylation in rice development and
221 responses to salt stress, we generated transgenic lines overexpressing SLR1
222 (SLR1-OX), as well as lines constitutively expressing a mimicry of the SUMOylated
223 form of SRL1 (SUMO1SLR1-OX) originated from the genetic fusion of mature
224 SUMO1 to the K2 residue, which is the SUMOylated lysine of SLR1
225 ($SUMO1_{GG}$::$SLR1_{K2}$) (Figure 3A). The strategy of using SUMOylated mimetic
226 isoforms originated by gene fusion with the SUMO coding sequence has been used
227 in several biological systems, including plants (Crozet et al., 2015; Ulrich, 2008). We
228 confirmed the overexpression of non-SUMOylated SLR1 isoforms in both SLR1-OX
229 and SUMO1SLR1, with the latter also showing a band with the expected mobility-
230 shift of SLR1 corresponding to mono-SUMOylation (Figure 3B). We also observed
231 an increase in the amount of non-SUMOylated SLR1 protein in SUMO1SLR1-OX
232 compared to WT and NS lines, which could be arising from the processing by
233 endogenous SUMO proteases because the fusion protein retains the SUMO
234 diglycine protease cleavage motif (-GGK-).

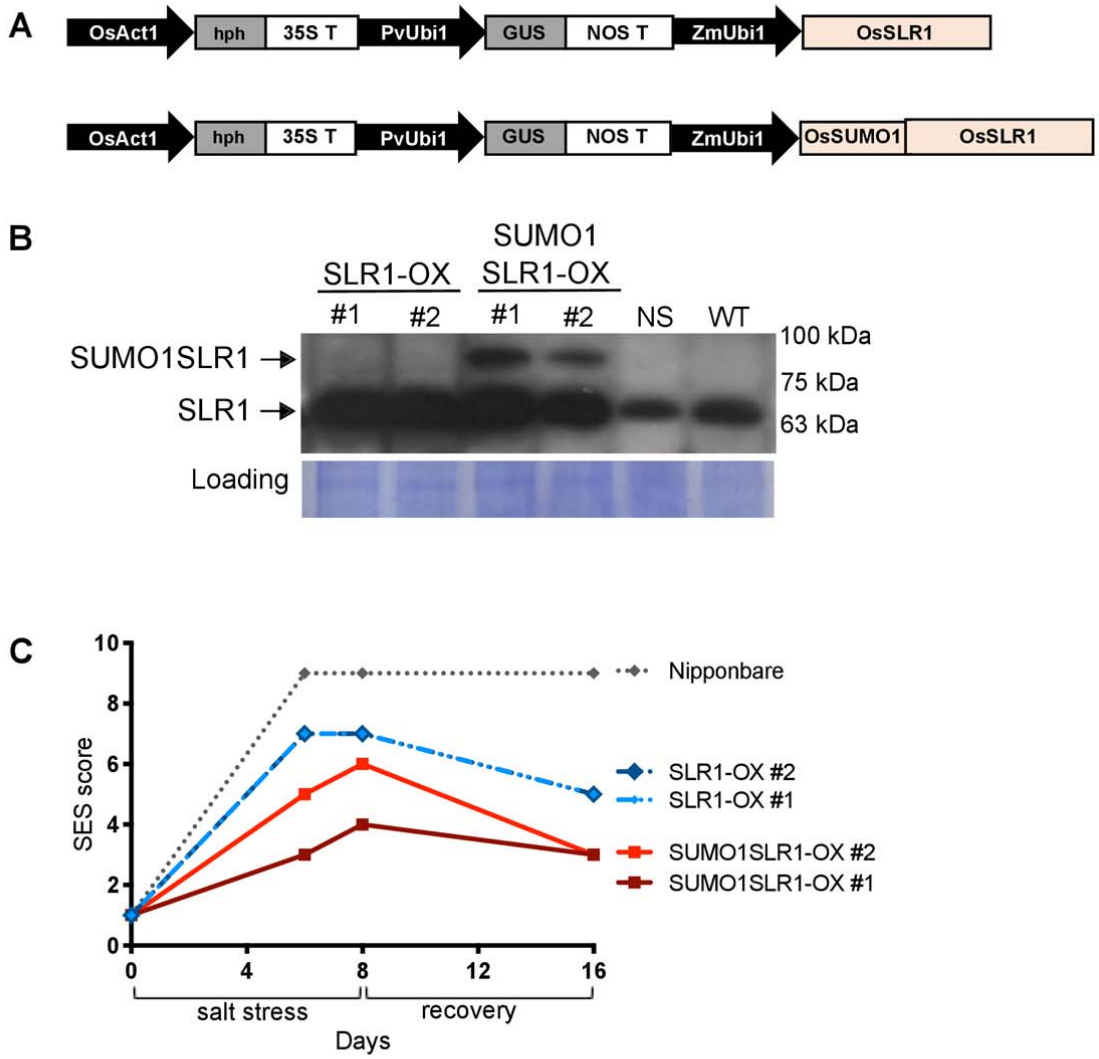

Figure 3. SLR1 SUMOylation confers salt tolerance at the seedling stage. (A) Depiction of gene constructs used to generate rice SLR1-OX and SUMO1SLR1-OX transgenic lines. *Zea mays* Ubi1 (ZmUbi1) promoter drives the expression of both OsSLR1 (SLR1-OX) and OsSLR1-OsSUMO1 gene fusion (SUMO1SLR1-OX). **(B)** SLR1 and SUMO1SLR1 protein accumulation in T2 independent transgenic lines (#1 and #2) of SUMO1SLR1-OX and SLR1-OX as detected by immunoblot using custom made anti-SLR1 antibody. **(C)** Stress severity as evaluated by IRRI salinity trial SES score for all lines in 6 and 8 days of stress and after 8 days of recovery period.

235 Rice is particularly sensitive to salt at both seedling and booting stages
236 (Gregorio et al., 1997). Therefore, we analysed stress marker symptoms of SLR1-
237 OX and SUMO1SLR1-OX lines subjected to high salt concentrations at seedling
238 stage, as well as yield parameters on salt treatments at booting stage. Evaluation of
239 symptoms in seedlings subjected to severe salinity (120mM NaCl) for 8 days showed
240 that both SUMO1SLR1-OX lines performed better under salt stress, displaying
241 decreased symptoms severity according to SES score (Standard Evaluation System

242 for Rice) by IRRI (International Rice Research Institute) (Gregorio et al., 1997),
243 including minimal leaf tip rolling and increased survival (Figure 3C). Importantly, salt
244 tolerance could be correlated with SUMOylated SLR1 levels, as SUMO1SLR1-OX
245 #1 – showing higher SLR1 SUMOylation levels compared to SUMO1SLR1-OX #2 –
246 performed better than the latter (Figure 3B-C). Interestingly, salt-induced
247 SUMOylated SLR1 increased alongside with the non-SUMOylated SLR1 in
248 SUMO1SLR1-OX lines (Supplemental Figure S3B), suggesting that SUMO cleavage
249 processing could be occurring alongside the duration of salt stress. Plants
250 overexpressing SUMO1SLR1 and SLR1-OX also recovered better than the wild type
251 Nipponbare in the 8 following days to salt stress cessation. Thus, mild
252 overexpression of SLR1 can increase rice tolerance to salinity, and this effect is
253 increased by its SUMOylation.

254 We next tested rice performance under salt stress at the booting stage.
255 Panicle initiation was the cue for mild salt stress imposition (80 mM NaCl), as at this
256 developmental stage pollen viability is most affected by high salinity (Negrão et al.,
257 2011; Sarhadi et al., 2012). Upon measurement of agronomical parameters, we did
258 not detect stress-induced changes in plant height (Figure 4A), tillering or panicle
259 length (Supplemental Figure S4) when compared to the control. However, two
260 critically important parameters for rice yield – namely fertility (filled grains) and
261 productivity (grain weight) – were significantly improved in SUMO1SLR1-OX lines
262 under mild salt stress. Both SLR1-OX and Nipponbare presented around 10%
263 decrease in fertility when comparing to mock conditions, while SUMO1SLR1-OX
264 showed the same fertility in both salt and mock treatments (Figure 4B). This
265 tendency was also observed in grain weight, where SUMO1SLR1-OX presented
266 higher tolerance to mild salt stress regarding productivity compared to Nipponbare
267 and SLR1-OX (Figure 4C). Although the SUMO1SLR1-OX lines had lower
268 productivity under mock conditions compared to Nipponbare, they showed improved
269 performance under salt stress. These results substantiate the significance of
270 SUMOylation of SLR1 in salt stress tolerance acquisition and yield protection
271 observed in two sensitive rice developmental stages.

272

273 **SLR1 SUMOylation regulates GA biosynthetic pathway transcripts in response**
274 **to salt stress**

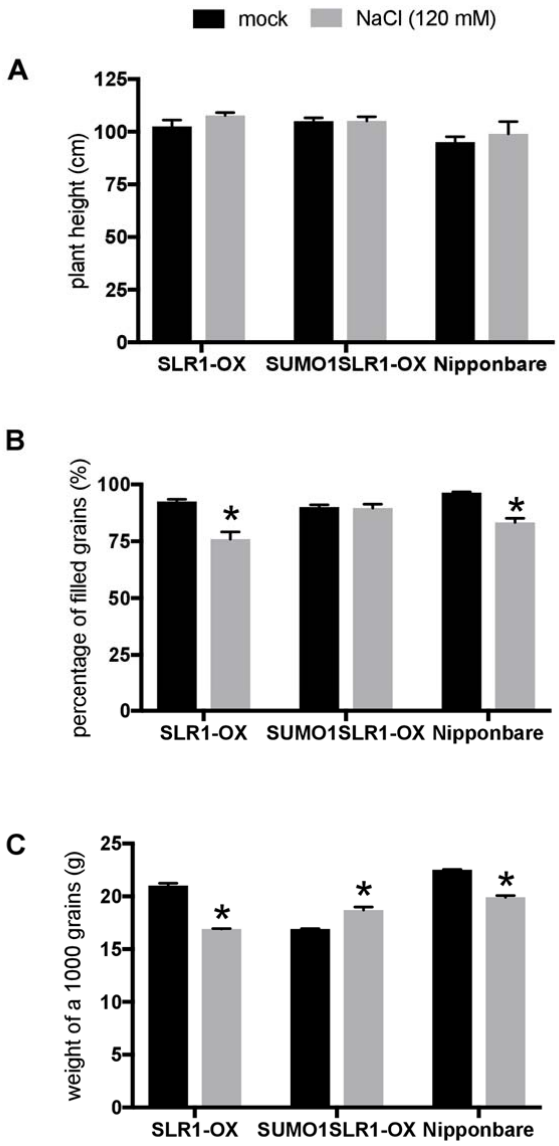

Figure 4. SLR1 SUMOylation reduces the impact of salt stress on yield. Agronomic parameters as measured at the end of rice life cycle: **(A)** plant height (N=6) **(B)** fertility as evaluated by the number of filled grains ratio to total panicle flowers (n>10) and **(C)** productivity as evaluated by the weight of 1000 grains (n>10). Error bars correspond to standard error (SE; 2 independent biological replicates with N=6 each) and statistically significant p-values represented as *($p<0.05$).

275 The salt tolerance observed in SUMO1SLR1-OX lines could not be attributed
276 to the increased accumulation of SLR1, as SLR1 protein levels were similar in the
277 SLR1-OX and SUMO1SLR1-OX transgenic lines (Figure 3B). Thus, we inferred that
278 the observed phenotypes in SUMO1SLR1-OX lines could be a consequence of the
279 increased levels of SUMOylated SLR1. Because DELLA proteins regulate
280 transcription, we performed a genome-wide expression analysis to identify

differentially regulated genes in SLR1-OX and SUMO1SLR1-OX that could explain the phenotypical differences observed in these lines in response to salt stress. We exposed SLR1-OX, SUMO1SLR1-OX, and Nipponbare genetic background to high salt concentrations (120 mM NaCl) during 8 hours at the seedling stage (2 weeks old), and collected samples for subsequent RNA-seq analysis (Supplemental Table S1). We selected the lines SLR1-OX #2 and SUMO1SLR1-OX #2 for the RNA-seq assay because they showed similar non-SUMOylated SLR1 levels, as we aimed to tackle the effect of SLR1 SUMOylation on gene expression. Both overexpressor lines showed an approximately 1.8-fold increase in SLR1 transcript levels when compared to Nipponbare, which is in line with the levels validated by real-time qPCR for the same samples, *ca.* 1.5-fold increase (Supplemental Figure S5), and with protein levels assessed by immunoblotting (Figure 3B). The induction of salt-induced genes *Rab21* and *P5CS* was used as a transcriptional readout of the salt stress treatment efficiency (Supplemental Figure S5).

Principal Component Analysis (PCA) revealed a clear separation of samples by treatment, this factor being responsible for 47% of the variability in gene expression, while genotype-specific transcriptomic changes explained 21% of the observed variability (Supplemental Figure S6). The constitutive overexpression of SLR1 and SUMO1SLR1 in absence of salt stress resulted in differential regulation of 247 and 207 genes, respectively (Supplemental Tables S1.6 to S1.8). Functional annotation of SLR1-OX DEGs showed enrichment of gene ontology (GO) terms associated with diterpenoid biosynthesis, highlighting the impact of SLR1 on GA metabolism (Supplemental Figure 7A and Supplemental Tables S1.6 to S1.7). Notably, we observed overall downregulation in genes coding for enzymes essential in non-gibberellin diterpenoid synthesis, namely syn-copalyl diphosphate synthase (*CPS4*) and ent-cassa-12,15-diene synthase (*KSL7*) (Supplemental Figures S7A and S7C). These enzymes are part of a diterpenoid pathway branching point that feeds the phytoalexins biosynthetic pathway (Otomo et al., 2004). Concurrently, other genes related to phytoalexin and phytocassane synthesis, such as cytochrome P450 family members *CYP701A8/KO1, CYP99A3, CYP71Z6, CYP76M8,* and *CYP71Z7*, were also downregulated in SLR1-OX.

Phenotypical discrimination of SLR-OX and SUMO1SLR1-OX was observed under salt stress but not under control conditions (Figure 3C). Interestingly, a closer look into the distribution of SLR-OX and SUMO1SLR1-OX samples in the PCA,

315 under control and stress conditions highlights a similar tendency (Supplemental
316 Figure S6). Hence, we focused on the analysis on the 236 DEGs specific to
317 SUMO1SLR1-OX exposed to salt stress. After functional annotation of DEGs
318 specific to SUMO1SLR1-OX, we found a significant over-representation of GO terms
319 associated with defence response and gibberellin dioxygenase activity
320 (Supplemental Figures S7B and S7C). We also found a salt stress-dependent
321 induction of *GA20ox2* and *GA2ox3* genes in SUMO1SLR1-OX (Supplemental Table
322 S1.4). *GA20ox2* and *GA2ox3* encode enzymes involved in the regulation of active
323 GA (GA_4) levels. Therefore, it is reasonable to hypothesize that SLR1 SUMOylation
324 could adjust active GA homeostasis upon exposure to salt stress (Supplemental
325 Figure S7C).
326
327 **SUMOylation disrupts SLR1 interaction with stress-associated transcription**
328 **factors**
329 The increased salt tolerance and sustained productivity of SUMO1SLR1-OX
330 under salt stress likely arise from the presence of increased levels of SUMOylated
331 SLR1 (Figure 3B-C; Figure 4A-B), which seems to be affecting the gene expression
332 profile of plants exposed to stress. The *GA20ox2* transcript was induced around 2-
333 fold in SUMO1SLR1-OX exposed to salt stress, while it showed only a marginal
334 induction in SLR1-OX under the same conditions (Supplemental Table S1.2). One
335 possible mechanism by which SLR1 could affect *GA20ox2* transcription is through
336 the interaction with the transcription factor YAB4, thereby repressing the expression
337 of *GA20ox2* (Yang et al., 2016). We did not detect *YAB4* transcript changes after 8
338 hours of salt stress exposure, but a search in public transcriptome data revealed that
339 *YAB4* is induced in rice shoots after 3h of salt stress imposition (Genevestigator -
340 Hruz et al., 2008; Supplemental Figure S8A-B), which could lead to increased YAB4
341 protein accumulation during later stages of plant adaptation to salt stress. In an
342 attempt to dissect the molecular pathways involved in *GA20ox2* upregulation in
343 SUMO1SLR1-OX, we verified the interaction of SLR1 and SUMOylated SLR1 with
344 YAB4 TF using a yeast two-hybrid system and bimolecular fluorescence
345 complementation (BiFC). The aim was to test the effect of SUMOylation on SLR1-
346 YAB4 interaction, which could affect *GA20ox2* transcription. We used a variant of the
347 SUMO1SLR1 fusion protein lacking the SUMO protease recognition domain to avoid
348 possible processing by yeast SUMO proteases (SUMO1($_{GG\text{-}AA}$)::SLR1). We

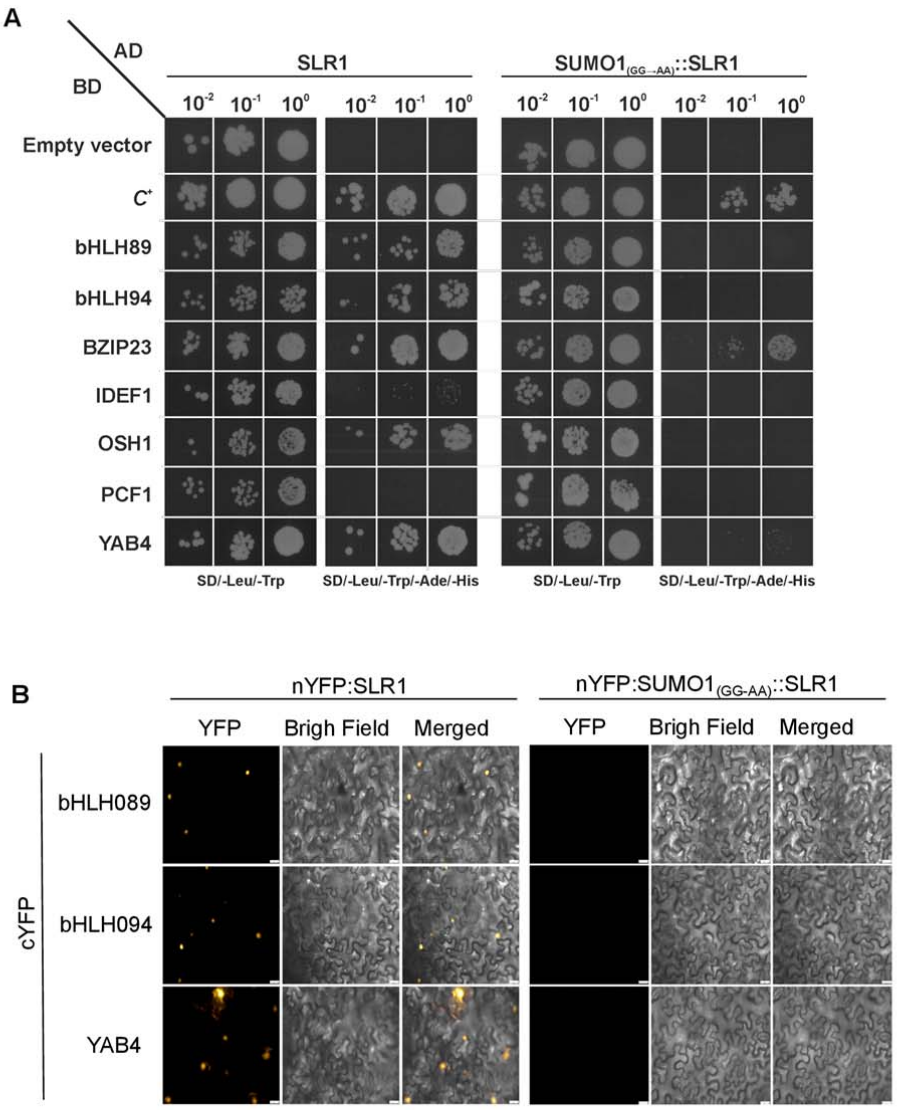

Figure 5. SLR1 SUMOylation affects its interaction with key transcription factors **(A)** Yeast-two hybrid (Y2H) analysis of both SLR1 and SUMO1SLR1. SUMO1::SLR1 fusion carries two mutations in the SUMO-protease cleavage motif (GG → AA) to avoid its removal by endogenous yeast proteases and guarantee constitutive SUMO attachment to SLR1 during the assay. Positive controls marked as (SD/-Leu/-Trip) and positive interactions marked with (SD/-Leu/-Trip/-Ade/-His) with C+ as an confirmed positive interaction control. **(B)** Bimolecular fluorescent complementation (BiFC) assays showing positive interactions between nYFP: SLR1 with cYFP:BHLH089, cYFP:BHLH094, and cYFP:YAB4. The presence of SUMO1 attached to lysine 2 of SLR1 (nYFP:SUMO1$_{(GG\text{-}AA)}$::SLR1) disrupts SLR1 interaction with these transcription factors. Negative controls for Y2H and BiFC assays can be found in Supplementary Figure S9.

349 confirmed the previously demonstrated interaction between SLR1 and YAB4 (Yang
350 et al., 2016), and also found that the presence of SUMO in lysine 2 of SLR1 disrupts
351 SLR1-YAB4 interaction in both yeast and *in planta* (Figure 5A-B; negative controls in
352 Supplementary Figure S9). The blocking of the SLR1 interaction with YAB4 by

353 SUMO correlates with the induction of *GA20ox2* in salt-stressed SUMO1SLR1-OX
354 lines.
355 To further evaluate the molecular aspects of SUMO1SLR1-OX tolerance to
356 salt stress, we explored the notion that SLR1 exerts its function mainly by
357 transcriptional regulation through interaction with transcription factors. We designed
358 a strategy that allowed us to identify SLR1 TF interactors that could explain, at least
359 partially, the differences in gene expression observed in the transgenic lines upon
360 exposure to salt stress. Briefly, we submitted the promoter sequences (1000 bp
361 upstream to the Transcription Start Site – TSS) of 417 selected DEGs (SLR1- and
362 SUMO1SLR1-dependent salt stress responsive genes; Supplemental Tables S1.3
363 and S1.4) to an *in silico* search for transcription factor binding sites (TFBS) in the
364 PlantPAN online database (Chow et al., 2016). Next, we selected only TFBS and
365 corresponding binding TFs that have been experimentally validated. This allowed us
366 to identify TFs from the TCP, bZIP, bHLH, and B3 families that could be regulating
367 the output gene expression of SLR1-OX and SUMO1SLR1-OX transgenic lines
368 under salt stress (Table 1). To cross-validate the TF identification, we made sure that
369 a substantial overlap between the known target genes of those TFs and the SLR1-
370 and SUMO1SLR1-dependent DEGs were observed (Supplemental Tables S1 and
371 S2).
372 The interaction between SLR1 with the selected candidates (Table 1) and its
373 regulation by SUMOylation was assessed through Y2H assays and BiFC analyses
374 (Figure 5A-B). The basic helix-loop-helix transcription factors bHLH089 and
375 bHLH094, as well as the homeobox TF OSH1, showed a strong interaction with
376 SLR1 but not with SUMO1($_{GG-AA}$)::SLR1. This finding suggests that SUMOylation
377 could modulate the binding of SLR1 to these transcription factors, potentially
378 affecting their transcriptional activities. We also found that BZIP23 can interact with
379 both SUMOylated and non-SUMOylated SLR1 (Figure 5A). The interaction of SLR1
380 with BHLH089 and BHLH094, as well as its disruption by SLR1 SUMOylation, was
381 validated through BiFC in *Nicotiana benthamiana* leaves, supporting the *in planta*
382 SUMO-dependent regulation of these interactions (Figure 5B). Neither IDEF1 nor
383 PCF1 showed interactions with SLR1 or SUMO1($_{GG-AA}$)::SLR1.
384
385

386 **DISCUSSION**
387

388 DELLA proteins are central regulators of plant productivity and stress
389 responses, and the hormonal crosstalk mediated by these proteins is essential for
390 plant plasticity to endure stress. As other hormone modulators, DELLA activity is
391 regulated by post-translational modifications, such as ubiquitination, phosphorylation,
392 *O*-fucosylation, *O*-GlcNAcylation, and SUMOylation (Yano et al., 2019; Zentella et
393 al., 2016; Zentella et al., 2017; Conti et al., 2014; Dai and Xue, 2010; Itoh et al.,
394 2003). Recently, SUMO proteases were linked to salt stress response in rice
395 (Srivastava et al., 2016b; 2017). Although deSUMOylation was proposed as a
396 general mechanism of tolerance acquisition in response to salt, we show that
397 artificially SUMOylated SLR1 could alleviate the salt stress impact on rice
398 productivity, also improving recovery after stress imposition is released.

399 Following the evidence that SUMO proteases are important for DELLA activity
400 (Campanaro et al., 2016), the knockout mutant of SUMO protease *fug1* showed a
401 higher ratio of overall SUMOylated SLR1. Interestingly, the FUG subclass is
402 phylogenetically close to the SPF subclass, which contains Ulp2-like SUMO
403 proteases (Castro et al., 2018). A Ulp2 from *Saccharomyces cerevisiae* (ScUlp2)
404 was previously reported to be the key protease responsible for poly-SUMO chain
405 processing (Eckhoff and Dohmen, 2015). If FUG1 is indeed related to Ulp2
406 proteases and it processes SUMO-SLR1, SLR1 deSUMOylation may be occurring in
407 poly-SUMO chain high molecular weight conjugates.

408 DELLA proteins control several plant processes through interaction with a
409 myriad of transcriptional factors (Van De Velde et al., 2017). By affecting protein-
410 protein interaction, SLR1 SUMOylation has the potential to modulate plant processes
411 by altering the transcriptional outcome of SLR1-TFs interacting proteins. Indeed,
412 transcriptomic analysis of SUMOylated SLR1 overexpressing lines suggested that
413 this isoform plays a role in early transcriptional responses to salt stress, affecting the
414 expression of key genes coding for enzymes controlling the accumulation of active
415 GA, such as *GA20ox2* and *GA2ox3*, involved in activation and inactivation of the
416 active GA_4. We were able to determine that SLR1 SUMOylation occurs in lysine 2
417 (Figure 1A-C), distant from the conserved GA regulatory domains DELLA and
418 TVHYNP. This finding suggests that SLR1 SUMOylation contrasts with Arabidopsis
419 RGA, in which the amino acid residue responsible for SUMO modification is the

420 lysine 65 (Conti et al., 2014), located very close to the GA-regulatory domain
421 TVHYNP. The location of SUMO attachment in SLR1 protein could exert quite
422 different effects on protein-protein interactions compared to its well-described
423 Arabidopsis counterpart RGA. An interesting possibility is that SUMOylation of these
424 residues could have a different outcome regarding the transcriptional activation
425 properties of SLR1 DELLA/TVHYNP motifs (Hirano et al., 2012). Both lysines are
426 within SUMOylation canonical motifs, but while the SUMOylation canonical motif
427 surrounding K2 is conserved in all analysed DELLAs, the one containing K65 is
428 exclusive to RGA. The different SUMOylation sites of SLR1 and RGA might account
429 for alterations in DELLA regulation amongst species that probably determine
430 different interactome networks.

431 The SUMOylation of SLR1 could also be affecting the interaction with
432 upstream regulatory proteins. For instance, SUMO attachment could affect SLR1
433 interaction with SPY, which enhances SLR1 activity through *O*-fucosylation and is a
434 major determinant of rice plant architecture (Yano et al., 2019). Crosstalk between
435 SUMOylation and *O*-fucosylation could play a role in GA-promoted growth regulation
436 by decreasing TF-interactions that result in growth repression (Camut et al., 2017).
437 This control of the expression of GA enzymes is demonstrated by our transcriptomic
438 results of SUMO1SLR1-OX lines under salt stress, which shows upregulation of both
439 *GA20ox2* and *GA2ox3*, suggesting that SLR1 SUMOylation could also regulate GA
440 homeostasis.

441 SUMOylation of specific targets was suggested to be crucial for stress
442 tolerance, fertility and yield maintenance in rice. For instance, BZIP63 SUMOylation
443 levels are modulated by OTS1, which affects its stability and the plant's ability to deal
444 with drought and salt stress (Srivastava et al., 2017). Interestingly, we found that
445 BZIP23 interacts with both SLR1 and SUMO1SLR1. Another novel interaction with
446 both bHLH089 and bHLH094 shows upregulation of JAZ-like repressors like JAZ8,
447 consistent with findings that this TF is regulating genes from the JA pathway as
448 observed in our transcriptomic analysis. Both these interactions may partly explain
449 the JA-induced stress response promoted by SLR1 accumulation (Supplemental
450 Figures S7A and S7B).

451 It was already shown that YAB4 interacts with SLR1 to repress *GA20ox2*
452 gene expression and restrain development in rice (Yang et al., 2016). We confirmed
453 the interaction between SLR1 and YAB4 by Y2H assays and BiFC (Figure 5B-C).

454 We additionally show that SUMOylation of SLR1 abolished its interaction with YAB4.
455 Accordingly, we found a stress-induced upregulation of *GA20ox2* in SUMO1SLR1-
456 OX (Supplemental Table S1). Moreover, *GA20ox2* was also found to be
457 downregulated by KNOTTED1-like homeobox (KNOX) proteins like OSH1
458 (Sakamoto et al., 2006). SLR1 SUMOylation also disrupted its interaction with
459 OSH1, suggesting that SLR1 SUMOylation mechanistic action is partly achieved
460 through SLR1 dissociation from transcriptional regulators involved in GA signalling
461 and stress signalling. It could represent a dissociation of DELLA function during salt
462 stress tolerance from its impact on productivity by means of SUMOylation.
463 The emergence of SUMOylation of SLR1 as an effector of rice tolerance to
464 salt stress, through the growth-maintaining modulation of protein-protein interaction
465 with transcriptional regulators such as YAB4, is evidence of the tight regulation of the
466 GA pathway by rice DELLA during stress. Recent studies have demonstrated that
467 DELLA proteins are targets of different post-translational modifications, which could
468 adjust their interactions with transcriptional regulators in a dynamic fashion, ensuring
469 the best developmental decisions when facing stress. Further studies need to be
470 performed to unveil upstream effectors that perceive stress and the underlying signal
471 transduction pathway that leads to SLR1 SUMOylation. By establishing the trigger
472 for SLR1 SUMOylation and its effect on stress-induced SLR1 protein-protein
473 interactions, new strategies can be developed involving the transient post-
474 translational modification of DELLA, as mutagenesis and selection of growth-
475 favourable SLR1 alleles. This can be used to activate the SUMO-regulated tolerance
476 mechanism when stress is forthcoming and protect crops from yield losses due to
477 abiotic stress.
478
479

480 **METHODS**

481 **SLR1 genomic DNA cloning and vectors construction**

482 The intronless gene SLR1 entire coding sequence was amplified from Nipponbare
483 wild-type genomic DNA, using the primers SLR1-CDS-Fw and SLR1-CDS-Rv
484 (Supplemental Table S4). The fragment was cloned into the pJET 1.2/blunt-end
485 cloning vector (ThermoScientific), and the SLR1 full sequence confirmed by Sanger
486 sequencing. SLR1 CDS was then amplified from pJET-SLR1 using the primers pET-
487 Fw-*Eco*RI and pET-Rv-*Psp*OMI (Supplemental Table S4) to insert the restriction
488 sites for *Eco*RI and *Psp*OMI to clone SLR1 in the pET28a expression vector
489 (Novagen). For the generation of rice transgenic lines overexpressing SLR1, the
490 SLR1 coding sequence was amplified from pJET-SLR1 using OsSLR1-GW-Fw and
491 OsSLR1-GW-Fw primers to insert the attB1 and attB2 recombination sites. The
492 amplified PCR-product was recombined into the pDONR221 (ThermoFisher).The
493 SUMO1SLR1 gene fusion was generated using high-fidelity PCR (Phusion DNA
494 Polymerase; NEB) essentially as described in Atanassov et al. (2009). Primers
495 overlapping both the OsSUMO1 3'-end and OsSLR1 5'-end OL-SLR1+SUMO1-3'-
496 Fw and OL SUMO1+SLR1-5'-Rv, were used in combination with OsSLR1-Gw-Rv
497 and OsSUMO1-GW-Fw, respectively, to generate the fragments to be fused. In the
498 next step, the PCR products were purified and used in the fusion PCR reaction
499 containing the OsSUMO1-GW-Fw and OsSLR1-Gw-Rv primers for the final
500 amplification of the final fusion product (Supplemental Table S4). The gene fusions
501 were confirmed by Sanger sequencing. To obtain rice transgenic plant lines
502 overexpressing SLR1 (SLR1-OX) and SLR1 fused to SUMO1 (SUMO1SLR1-OX),
503 pDONR221 containing the inserts described above was used as entry vector for the
504 pANIC6B destination vector (Mann et al., 2011). The expression of SLR1 and
505 SUMO1SLR1 is controlled by the maize *ZmUbi1* promoter (Figure 3A).

506

507 **Site-directed mutagenesis**

508 For the production of truncated recombinant SLR1 protein (SLR1t) containing the
509 leading 190 amino acid residues of SLR1, a stop codon was introduced by site-
510 directed mutagenesis (SDM) in pET28a-SLR1 using *Pfu*Turbo DNA polymerase
511 (Agilent) and the primers (SLR1t-STOP-Fw and SLR1t-STOP-Rv) designed with
512 QuickChangeII online tool (Agilent) (Supplemental Table S4). Unmodified plasmids
513 were digested with methylation-sensitive enzyme *Dpn*I (New England Biolabs). The

514 mutated plasmids were transformed in *E. coli* DH5α and the mutagenized site
515 confirmed by sequencing. Mutated pET28a coding the truncated SLR1 isoform
516 (SLR1t) was subjected to further mutagenesis procedures to perform the amino acid
517 substitutions K2R and K60R (primers SLR1t-K2R-Fw, SLR1t-K2R-Rv, SLR1t-K60R-
518 Fw and SLR1t-K60R-Rv, all listed in Supplemental Table S4) following the same
519 protocol.
520
521 **Recombinant Protein Production and Purification**
522 pET28a vectors containing the full-length SLR1, N-terminus truncated SLR1 (SLR1t),
523 SLR1t (K2R) and SLR1t (K60R) were transformed into *E. coli* strain BL21 Star (DE3,
524 Sigma-Aldrich) for recombinant protein expression. Cells were grown at 37ºC until
525 OD_{600} = 0.6, and protein production was induced by addition of 200 µM isopropyl-d-
526 1-thiogalactopyranoside (IPTG). After three hours, the cells were harvested by
527 centrifugation in a J2MI centrifuge (Beckman) at 7000 RPM during 20 minutes at
528 4ºC. The cells were resuspended in lysis buffer (phosphate buffer 20 mM pH 7.5,
529 500 mM NaCl, 10 mM Imidazole) containing 5 µg/mL of DNAse, 50 µg/mL of
530 lysozyme, PMSF 100 mM and $MgCl_2$ 25 mM. After freezing at -20ºC and thawing,
531 extracts were loaded into a HisTrap chelating column (Amersham Biosciences) and
532 proteins eluted in phosphate buffer containing 500 mM imidazole, following buffer
533 exchange dialysis (phosphate buffer 20 mM, NaCl 150 mM, DTT 1 M, glycerol 2%),
534 for increased protein stability. Recombinant proteins were analysed by Western Blot
535 using custom-made SLR1 specific polyclonal antibody with Mini-Protean II system
536 (Biorad).
537
538 ***In vitro* SUMOylation assays and ULP1 treatment**
539 The *in vitro* SUMOylation assays were performed in 20 µL of SUMOylation reaction
540 buffer (Werner et al., 2009) containing 3 µg of SLR1 recombinant protein, 1 µg of E1-
541 activating enzyme (OsSAE1/ OsSAE2), 0.8 µg of E2-conjugating enzyme
542 (OsSCE1a), 0.5 µg of OsSUMO1/2, 0.4 units of creatine phosphokinase, and 10 mM
543 creatine phosphate. Reactions were initiated by adding 1 mM ATP and then
544 incubated at 37ºC for 1 h to 3 h. To confirm SUMOylation specificity, 3 µg of purified
545 SUMO protease ULP1 from *Saccharomyces cerevisiae* (Li and Hochstrasser, 2003)
546 was used for deSUMOylation analysis. SUMO conjugates were analysed by Western

547 Blot with custom anti-SLR1 antibody. For ULP1 treatments, whole plants were
548 ground in liquid N_2 and 100 mg of ground tissue powder were mixed with non-
549 denaturing buffer (Tris-HCl pH 8.0 50 mM, sodium chloride 150 mM, NP-40 1%,
550 sodium deoxycholate 0.5%, SDS 0.1%, EDTA pH 8.0 1 mM, NEM 50 mM), followed
551 by homogenisation by vortexing, and subsequent centrifugation at 4 ºC for 20
552 minutes to recover the supernatant containing the proteins. The non-denaturing
553 protein extracts were treated with 7 µg of ULP1, incubated at 37 ºC with collection
554 points taken at 5, 30, 60, and 120 seconds. Proteins were denatured at 90ºC for 10
555 minutes with Laemmli Buffer with 5 mM DTT and anti-SLR1 immunoblot proceeded
556 as described above.
557
558 **SLR1 protein extraction, detection and quantification analysis**
559 Plant shoot samples were ground in liquid N_2 and 100 mg of ground tissue used for
560 protein extraction with denaturing TCA/Acetone precipitation, followed by
561 resuspension in lysis buffer (7 M Urea, 2 M Thiourea, 30 mM Tris, 4% (w/v) CHAPS,
562 4 % (v/v), cOmplete protease inhibitor cocktail EDTA-Free (Sigma-Aldrich), 0.1%
563 (v/v) Nuclease Mix 100x, and NEM 20 mM. Protein quantification was performed with
564 2-D Quant kit (GE Healthcare) following manufacturer's instructions. Anti-SLR1
565 immunoblots were performed in a Mini-Protean II System (Biorad), using custom-
566 made anti-SLR1 polyclonal specific antibody [1:5.000, overnight incubation] and anti-
567 rabbit (Novex) [1:20.000, 90 min incubation] in 5% non-fat dry milk in TBS 1X.
568 Quantification of native SLR1 bands provided by immunoblotting analysis,
569 normalized to protein loading control using stripped membrane stained with
570 Coomassie G-250 (Fluka), was performed with ImageJ software as indicated in the
571 official ImageJ website online tutorial.
572
573 **Plant material and Rice transformation**
574 Calluses induced from wild-type *Oryza sativa* (japonica spp.) cv. Nipponbare mature
575 seeds were used for rice transformations according to (Almadanim et al., 2017), and
576 selection for transformants asserted by hygromycin resistance and standard GUS-
577 staining with X-Gluc solution (Roth) of a section of seminal roots. Proteins were
578 extracted, detected and quantified using a modified TCA/Acetone method (Luís et
579 al., 2016). Due to growth arrest phenotype and fertility decrease in homozygous lines
580 of SUMO1SLR1-OX lines, all assays continued with positively-selected

581 heterozygous plants. Moreover, lines #2 for both SUMO1SLR1-OX and SLR1-OX
582 were selected for further analysis at rice booting stage and transcriptomic evaluation
583 according to non-SUMOylated SLR1 levels, in order to avoid DELLA pleiotropic
584 effects (Davière and Achard, 2015). Wild-type Nipponbare was used as a control for
585 SLR1-OX and SUMO1SLR1-OX obtained by transformation as described above.
586 N<egative segregant lines of Zhonghua and Hwayoung varieties were used as
587 controls for T-DNA insertion lines knock-out mutants for rice SUMO proteases ELS1
588 (04Z11JY66) and FUG1 (2A-20225 obtained from RMD (www.rmd.ncpgr.cn),
589 developed by the National Centre of Plant Gene Research) and Postech
590 (www.postech.ac.kr/life/pfg/risd, developed by Gynheung An), respectively. These
591 insertion line seeds were germinated, self-crossed and screened using PCR analysis
592 for homozygosity (Rosa et al., 2018). The T-DNA insertion position was determined
593 by sequencing. Gene expression was analysed by RT-qPCR (Rosa et al., 2018).
594
595 **Salinity Stress Assays**
596 For the assays performed at the seedling stage, heterozygous transgenic seeds
597 were germinated and selected through screening for hygromycin resistance and
598 GUS staining. Seedlings were transferred to hydroponics for salinity resistance
599 screening (Almeida et al., 2016) with half-strength Murashige & Skoog Medium and
600 MES buffer 250 mg/L (Duchefa) with pH adjusted to 5.2. Seedlings were grown for
601 14 days before the salt stress assay. Then, the seedlings were exposed to salt
602 stress, with electric conductivity (EC) set and maintained at 12 dS/m with sodium
603 chloride solution for the extension of the stress treatment. After 8 days, the seedlings
604 were transferred to regular medium for recovery. Stress severity (SES score) – 1 for
605 lower severity and 9 for higher severity - was evaluated as set by IRRI (Gregorio et
606 al., 1997) at 6 and 8 days after stress and 8 days after recovery. Samples for
607 transcriptomic analysis – 4 replicates of a pool of 3 plants - were collected at 8 hours
608 after the initiation of the salt stress, corresponding to 10 hours after the lights went
609 on, for both control and salt treatments, and frozen immediately in liquid nitrogen for
610 grinding and analysis. Samples from 0h, 2h, 4h, and 8h treatments were obtained
611 from shoots and roots collected separately, and frozen immediately in liquid nitrogen.
612 Protein was extracted, detected and quantified as described above. For the booting
613 stage assay, previously germinated and selected heterozygous transgenic seeds
614 were sown in pots with 2-parts soil, 2-parts peat, and 1-part vermiculite. The

615 experiment was set up in the greenhouse from June to September, according to IRRI
616 standard screening procedures (Gregorio et al., 1997). Genotypes were maintained
617 in separate containers, for both stress and control pots, to control for discrepancies
618 in panicle initiation times. Panicle initiation was evaluated by the emergence of the
619 flag-leaf with a distance between 1 and 2 cm to the adjacent leaf and salinity applied
620 individually for each genotype at that point. Electric conductivity (EC) was set and
621 maintained at 8 dS/m with sodium chloride solution for the extension of the life cycle.
622 Upon complete maturation of the seed, agronomical parameters were measured
623 (plant height, tillering, and panicle length) and panicles collected for further
624 characterization of fertility (analysing the number of full matured seeds to total
625 number of flowers ratio) and productivity (weight of 1000 seeds as measured in a
626 Pfeuffer seed counter). The significance of statistics was asserted by t-test with
627 Holm-Sidak method correction for multiple comparisons and a $p<0.05$ threshold.
628
629 **RNA Extraction and expression analysis**
630 RNA was extracted from a total of 100 mg of ground frozen shoot tissue with Direct-
631 zol kit (Zymo Research) according to manufacturer's protocol with in-column DNAse
632 treatment. The first-strand cDNA was synthesized from 2 µg of total RNA with an
633 anchored-oligo (dT)18 primer using the Transcriptor High Fidelity cDNA Synthesis
634 Kit (Roche) according to the manufacturer's instructions. Reverse Transcription
635 quantitative PCR (RT- qPCR) analysis was performed using a LightCycler 480
636 system (Roche) and the SYBR Green I Master mix (Roche). The RT-qPCR reactions
637 were carried out with the primers listed in Supplemental Table S4. PCR running
638 conditions were: one cycle at 95ºC for 5 min and 45 cycles of amplification at 95ºC
639 for 10 s, 56–60ºC for 10 s and 72ºC /10 s. The CT values were calculated using
640 three technical replicates, and gene expression was assessed relative to described
641 internal reference transcript controls, rice *UBIQUITIN CONJUGASE2* (OsUBC2) and
642 *UBIQUITIN10* (OsUBQ10) (Moraes et al., 2015; Pabuayon et al., 2016). For the
643 RNA-seq procedure, the small RNAs in the extracted total RNA samples were
644 cleaned by using the RNeasy spin column from RNeasy Mini Kit (Qiagen) following
645 RNA Cleanup protocol. RNA quality was assessed by Fragment Analyzer
646 (ThermoFisher) with RNA Quality Number over 5. A total of 18 cDNA libraries were
647 prepared, using three biological replicates for each genotype (SLR1-OX,
648 SUMO1SLR1-OX, Nipponbare) and each condition (mock and salt). Enzymatic

649 fragmentation with Pico Nextera kit and Smart-Seq2 multiplexed-library
650 preparation were performed[49] and single-end sequencing on NextSeq500 (Illumina)
651 with High Output Kit (75 cycles).
652
653 **RNA-seq Data Analysis**
654 Raw data FASTQ files were inputted on R/Bioconductor-based user interface
655 analysis software Chipster for RNA-seq. Single-end reads were trimmed with
656 PRINSEQ for 55 bp total with 18 bp trimmed on 5' end and quality control of 28% set
657 for the 3' end for adapter removal. Read alignment was performed with TOPHAT2
658 against the *Oryza sativa* genome (version IRGSP-1.0.36), selecting Sanger-Phred
659 +33 as quality score format. An average of 25.000.000 and 21.000.000 aligned and
660 uniquely mapped reads, respectively, were obtained per library (Supplemental Table
661 S2). For differential expression analysis, BAM files resulting from alignment were
662 submitted to pairwise comparisons with Cufflinks2 tool Cuffdiff for a set 0.05 False
663 Discovery Rate (5% FDR) with sequence-specific bias and multi-mapped read
664 corrections enabled. Differentially expressed genes (DEGs) with a 1.5 fold-change
665 were selected for data visualization and functional annotation using ClueGO plug-in
666 (Bindea et al., 2009) for Cytoscape (Su et al., 2014).
667
668 **Promoter Analysis and Interaction Validation by Y2H and BiFC**
669 The 1000 bp promoter region of differential expressed genes DEGs were
670 downloaded from Rice Annotation Project Database (RAP-DB) (Sakai et al., 2013)
671 and submitted to PlantPAN 2.0 (Chow et al., 2016) for *cis*-elements for transcription
672 factor binding site (TFBS) analysis. Gene Group Analysis was used to search for
673 common (90%) *cis*-element binding (TFBS) sites and the transcription factors (TFs)
674 associated with DEG promoters. Rice TFs were examined individually for
675 experimentally verified data concerning the interaction to binding sites and
676 downstream target genes listing (Supplemental Table S2). Resulting target genes
677 were then overlapped with previously verified DEGs from RNA-seq analysis. For the
678 Y2H assays, coding sequences of SLR1 and OsSUMO1($_{GG\text{-}AA}$)::SLR1 were cloned
679 into the pGADT7 vector (Stratagene, USA) while OsBHLH089, OsBHLH094,
680 OsBZIP23, OsIDEF1, OsOSH1, OsPCF1 and OsYAB4 were cloned into the
681 pGBKT7 (Stratagene, USA) vector. These constructs were transformed into
682 *Saccharomyces cerevisiae* strain Y2HGold (Clontech, US) applying the LiAc method.

683 Yeast transformed cells were plated on synthetic defined (SD) medium lacking
684 leucine and tryptophan for plasmid transformation control and in SD lacking leucine
685 (-Leu), tryptophan (-Trip), adenine (-Ade), and histidine (-His) for interaction
686 screening. The interactions were evaluated in three individual colonies transformed
687 with both plasmids. pAD-WT and pBD-WT from the HybriZAP 2.1 kit (Stratagene,
688 USA) were used as a control of positive interaction (C+). pGBKT7 and pGADT7
689 empty vectors were also co-transformed with pGADT7-SLR1, pGADT7-SUMO1($_{GG-}$
690 $_{AA}$)::SLR1 and pGBKT7-BHLH089, pGBKT7-BZIP23, pGBKT7-IDEF1, and pGBKT7-
691 YAB4, respectively, as negative controls. For bimolecular fluorescence
692 complementation (BiFC), OsSLR1, OsSUMO1($_{GG-AA}$)::SLR1 were cloned in YFN43,
693 and OsBHLH089, OsBHLH094 and OsYAB4 were cloned into YFC43 (Belda-
694 Palazón et al., 2012). *Nicotiana benthamiana* leaves were co-infiltrated with
695 *Agrobacterium tumefaciens* strain EH105 harbouring the appropriate vectors.
696 Fluorescence was visualized using the Leica DM6 B fluorescence microscope (40x)
697 with L5 filter cube (Leica, Germany) 48-72h following infiltration. As negative control,
698 YFN43 (empty vector) was also co-infiltrated with YFC43-BHLH089, YFC43-
699 BHLH094 and YFC43-YAB4. *Agrobacterium* expressing the viral silencing
700 suppressor P19 was included in all infiltrations to increase the expression in *N.*
701 *benthamiana* leaves. BiFC analyses were performed essentially as described in
702 Belda-Palazón et al., 2012.
703
704 **Accession Numbers**
705 Sequence data from this article can be found in the Rice Annotation Project
706 Database (RAP-DB) under the following accession numbers: OsSLR1
707 (Os03g0707600), OsSUMO1 (Os01g0918300), OsSUMO2 (Os01g0918200),
708 OsSAE1 (Os11g0497000), OsSCE1a (Os03g0123100), OsELS1 (Os01g0355900),
709 OsFUG1 (Os03g0344300), OsUBC2 (Os02g0634800), OsUBQ10 (Os06g0681400),
710 OsP5CS (Os05g0455500), OsRAB21 (Os11g0454300), RGA (At2g01570), OsCPS4
711 (Os04g0178300), OsKSL7 (Os02g0570400), OsCYP701A8/KO1 (Os06g0569500),
712 OsCYP99A3 (Os04g0178400), OsCYP71Z6 (Os02g0570500), OsCYP76M8
713 (Os02g0569400), OsCYP71Z7 (Os02g0570700), OsCKX2 (Os01g0197700),
714 OsCKX5 (Os01g0775400), OsLOX2 (Os08g0509100), OsCHT3 (Os06g0726100),
715 OsCHT8 (Os10g054290), OsCHT11 (Os03g0132900), OsGA20ox2
716 (Os01g0883800), OsGA2ox3 (Os01g0757200), OsPCF1 (Os04g0194600),

717 OsRISBZ3 (Os02g0266800), OsBHLH089 (Os03g0802900), OsBHLH094
718 (Os07g0193800), OsBZIP23 (Os02g0766700), OsOSH1 (Os03g0727000), OsPCF1
719 (Os03g0785800), OsIDEF1 (Os11g0175700), OsYAB4 (Os02g0643200).
720
721

Supplementary Materials

Figure S1. Alignment of DELLAs protein sequences of selected monocots and dicots.
Figure S2. SRL1 can be SUMOylated by both OsSUMO1 and OsSUMO2 *in vitro.*
Figure S3. Accumulation dynamics of SRL1 transcript and protein in response to salt stress.
Figure S4. Tillering and panicle length were not affected by mild salt stress imposition.
Figure S5. Analysis of salt treatment efficiency by salt-stress marker gene induction.
Figure S6. Salt treatment had a major contribution to the differences in gene expression among Nipponbare, SLR1-OX and SUMO1SLR1-OX.
Figure S7. Transcriptomics reveal differential stress-induced regulation by SUMOylated SLR1.
Figure S8. Genevestigator Results for Gene Expression of YABBY4 (LOC_Os02g4950) in Salinity Assays.
Figure S9. Protein-protein interaction (PPI) negative controls for Y2H and BiFC assays.
Table S1. RNA seq data showing >1.5 fold Differentially Expressed Genes in Nipponbare, SLR1-OX and SUMOSLR1-OX, in mock and salt stress conditions.
Table S2. Expression changes of selected putative SLR1 TF interactors (A) and the respective downstream target genes (B). Fold-change shown as $\log_2$ FC. Comparison of condition A with condition B corresponding to respective selected analysis in Cufflinks (FPKM1 x FPKM2, for condition A and B, respectively). Nipp-Nipponbare; (m)-mock; (s)-stress
Table S3. RNA-seq read count for each of the sequenced libraries and respective legend
Table S4. List of primers used for gene cloning, site directed mutagenesis (SDM) and gene expression quantification (RT-qPCR). Details for the use of specific primers are given in the text.

Acknowledgments

Portuguese Fundação para a Ciência e a Tecnologia (FCT) for fellowships for NMG (SFRH/BD/85799/2012), TF (PD/BD/135584/2018), MTGR (SFRH/BD/84219/2012), MAAR (SFRH/BD/87420/2012), PMB (SFRH/BPD/86742/2012). FCT Investigator IF/00764/2014 (POPH-QREN) for IAA and PTDC/BIA-FBT/31211/2017 for CM contract. Work was supported by P-KBBE/0001/2012 and also by the FCT research unit GREEN-it "Bioresources4sustainability" (UID/Multi/04551/2013 and UIDB/04551/2020). The funding sources had no involvement in study design, analyses, and interpretation of data, writing, or in the submission decision.

764 **Table 1. Enriched binding sites and associated transcription factors in SLR1**
765 **DEGs promoters.** Promoter sequence analysis output from PlantPAN with Support
766 referencing the percentage of transcription factor binding elements
767 (TFBS/Sequence) found in SLR1- and SUMO1SLR1-dependent stress-responsive
768 DEGs. Resulting TF overlap with DEGs detailed in Supplementary Table S4.
769

TFBS	Support	TF Family	TF	Annotation
GGTCCCAC	91.4	**TCP**	**PCF1/2**	essential for meristematic tissue-specificity expression of the PCNA gene promoter
TACGTA	91.4	**(Others)**	**RISBZ3**	found in seed storage protein gene promoters
GCACGTGC	94.7	**bHLH**	**BHLH089/094**	forms a ternary complex with RSS3 and TIFY11A/JAZ9 to negatively regulate jasmonate-responsive genes
ACACGTGT	97.4	**bZIP**	**BZIP23/46**	binds specifically to the abiotic stress ABA-responsive elements (ABRE) in the promoter of target genes
TNCGTACAA	98.0	**SBP**	**SPL1**	trans-acting factor that binds specifically to the consensus nucleotide sequence 5'-TNCGTACAA-3'
TGAC	98.7	**Homeobox**	**OSH1**	involved in shoot formation during embryogenesis
CATGC	100.0	**B3**	**IDEF1**	involved in iron deficiency response and tolerance
CCAAT	100.0	**NF-YB**	**NFBY1/2/3/4**	component of the NF-Y/HAP transcription factor complex regulating the expression of photosynthetic genes

770
771
772

Parsed Citations

Achard, P., Cheng, H., De Grauwe, L., Decat, J., Schoutteten, H., Moritz, T., Van Der Straeten, D., Peng, J., and Harberd, N.P. (2006). Integration of plant responses to environmentally activated phytohormonal signals. Science 311, 91–94.
Pubmed: Author and Title
Google Scholar: Author Only Title Only Author and Title

Almadanim, M.C., Alexandre, B.M., Rosa, M.T.G., Sapeta, H., Leitão, A.E., Ramalho, J.C., Lam, T.T., Negrão, S., Abreu, I.A., and Oliveira, M.M. (2017). Rice calcium-dependent protein kinase OsCPK17 targets plasma membrane intrinsic protein and sucrose-phosphate synthase and is required for a proper cold stress response. Plant Cell Environ. 40, 1197–1213.
Pubmed: Author and Title
Google Scholar: Author Only Title Only Author and Title

Almeida, D.M., Almadanim, M.C., Lourenço, T., Abreu, I.A., Saibo, N.J.M., and Oliveira, M.M. (2016). Screening for Abiotic Stress Tolerance in Rice: Salt, Cold, and Drought. In Environmental Responses in Plants, (New York, NY: Humana Press, New York, NY), pp. 155–182.
Pubmed: Author and Title
Google Scholar: Author Only Title Only Author and Title

Atanassov, I.I., Atanassov, I.I., Etchells, J., and Turner, S.R. (2009). A simple, flexible and efficient PCR-fusion/Gateway cloning procedure for gene fusion, site-directed mutagenesis, short sequence insertion and domain deletions and swaps. Plant Methods 2009 5:1 5, 14.
Pubmed: Author and Title
Google Scholar: Author Only Title Only Author and Title

Augustine, R.C. and Vierstra, R.D. (2018). SUMOylation: re-wiring the plant nucleus during stress and development. Current opinion in plant biology, 45, pp.143-154.
Pubmed: Author and Title
Google Scholar: Author Only Title Only Author and Title

Belda-Palazón, B., Ruiz, L., Martí, E., Tárraga, S., Tiburcio, A.F., Culiáñez, F., Farràs, R., Carrasco, P. and Ferrando, A. (2012). Aminopropyltransferases involved in polyamine biosynthesis localize preferentially in the nucleus of plant cells. PLoS One, 7(10), p.e46907.
Pubmed: Author and Title
Google Scholar: Author Only Title Only Author and Title

Bindea, G., Mlecnik, B., Hackl, H., Charoentong, P., Tosolini, M., Kirilovsky, A., Fridman, W.-H., Pagès, F., Trajanoski, Z., and Galon, J. (2009). ClueGO: a Cytoscape plug-in to decipher functionally grouped gene ontology and pathway annotation networks. Bioinformatics 25, 1091–1093.
Pubmed: Author and Title
Google Scholar: Author Only Title Only Author and Title

Campanaro, A., Battaglia, R., Galbiati, M., Sadanandom, A., Tonelli, C., and Conti, L. (2016). SUMO proteases OTS1 and 2 control filament elongation through a DELLA-dependent mechanism. Plant Reprod 29, 1–4.
Pubmed: Author and Title
Google Scholar: Author Only Title Only Author and Title

Camut, L., Davière, J.-M., and Achard, P. (2017). Dynamic Regulation of DELLA Protein Activity: SPINDLY and SECRET AGENT Unmasked! Mol Plant 10, 785–787.
Pubmed: Author and Title
Google Scholar: Author Only Title Only Author and Title

Castro, P.H., Bachmair, A., Bejarano, E.R., Coupland, G., Lois, L.M., Sadanandom, A., van den Burg, H.A., Vierstra, R.D., and Azevedo, H. (2018). Revised nomenclature and functional overview of the ULP gene family of plant deSUMOylating proteases. J. Exp. Bot. 69, 4505–4509.
Pubmed: Author and Title
Google Scholar: Author Only Title Only Author and Title

Chow, C.-N., Zheng, H.-Q., Wu, N.-Y., Chien, C.-H., Huang, H.-D., Lee, T.-Y., Chiang-Hsieh, Y.-F., Hou, P.-F., Yang, T.-Y., and Chang, W.-C. (2016). PlantPAN 2.0: an update of plant promoter analysis navigator for reconstructing transcriptional regulatory networks in plants. Nucleic Acids Research 44, D1154–D1160.
Pubmed: Author and Title
Google Scholar: Author Only Title Only Author and Title

Conti, L., Nelis, S., Zhang, C., Woodcock, A., Swarup, R., Galbiati, M., Tonelli, C., Napier, R., Hedden, P., Bennett, M., et al. (2014). Small Ubiquitin-like Modifier protein SUMO enables plants to control growth independently of the phytohormone gibberellin. Developmental Cell 28, 102–110.
Pubmed: Author and Title
Google Scholar: Author Only Title Only Author and Title

Cremona, C.A., Sarangi, P., and Zhao, X. (2012). Sumoylation and the DNA Damage Response. Biomolecules 2012, Vol. 2, Pages 376-388 2, 376–388.
Pubmed: Author and Title

Google Scholar: Author Only Title Only Author and Title

Crozet, P., Margalha, L., Butowt, R., Fernandes, N., Elias, C.A., Orosa, B., Tomanov, K., Teige, M., Bachmair, A., Sadanandom, A., et al. (2015). SUMOylation represses SnRK1 signaling in Arabidopsis. The Plant Journal 85, 120–133.
Pubmed: Author and Title
Google Scholar: Author Only Title Only Author and Title

Dai, C., and Xue, H.-W. (2010). Rice early flowering1, a CKI, phosphorylates DELLA protein SLR1 to negatively regulate gibberellin signalling. The EMBO Journal 29, 1916–1927.
Pubmed: Author and Title
Google Scholar: Author Only Title Only Author and Title

Davière, J.-M., and Achard, P. (2015). A pivotal role of DELLAs in regulating multiple hormone signals. Mol Plant 9, 10–20.
Pubmed: Author and Title
Google Scholar: Author Only Title Only Author and Title

de Lucas, M., Daviere, J.M., Rodriguez-Falcon, M., Pontin, M., Iglesias-Pedraz, J.M., Lorrain, S., Fankhauser, C., Blazquez, M.A., Titarenko, E., and Prat, S. (2008). A molecular framework for light and gibberellin control of cell elongation. Nature 451, 480-484.
Pubmed: Author and Title
Google Scholar: Author Only Title Only Author and Title

Eckhoff, J., and Dohmen, R.J. (2015). In Vitro Studies Reveal a Sequential Mode of Chain Processing by the Yeast SUMO (Small Ubiquitin-related Modifier)-specific Protease Ulp2. J. Biol. Chem. 290, 12268–12281.
Pubmed: Author and Title
Google Scholar: Author Only Title Only Author and Title

Fukazawa, J., Mori, M., Watanabe, S., Miyamoto, C., Ito, T., and Takahashi, Y. (2017). DELLA-GAF1 Complex Is a Main Component in Gibberellin Feedback Regulation of GA20 Oxidase 2. Plant Physiology 175, 1395–1406.
Pubmed: Author and Title
Google Scholar: Author Only Title Only Author and Title

Gregorio, G.B., Senadhira, D., and Mendoza, R.D. (1997). Screening rice for salinity tolerance. Irri.
Pubmed: Author and Title
Google Scholar: Author Only Title Only Author and Title

Hedden, P., and Thomas, S.G. (2012). Gibberellin biosynthesis and its regulation. Biochemical Journal 444, 11–25.
Pubmed: Author and Title
Google Scholar: Author Only Title Only Author and Title

Hirano, K., Asano, K., Tsuji, H., Kawamura, M., Mori, H., Kitano, H., Ueguchi-Tanaka, M., and Matsuoka, M. (2010). Characterization of the molecular mechanism underlying gibberellin perception complex formation in rice. The Plant Cell Online 22, 2680–2696.
Pubmed: Author and Title
Google Scholar: Author Only Title Only Author and Title

Hirano, K., Ueguchi-Tanaka, M., and Matsuoka, M. (2008). GID1-mediated gibberellin signaling in plants. Trends Plant Sci 13, 192–199.
Pubmed: Author and Title
Google Scholar: Author Only Title Only Author and Title

Hirano, K., Kouketu, E., Katoh, H., Aya, K., Ueguchi-Tanaka, M. and Matsuoka, M. (2012). The suppressive function of the rice DELLA protein SLR1 is dependent on its transcriptional activation activity. The Plant Journal, 71(3), pp.443-453.
Pubmed: Author and Title
Google Scholar: Author Only Title Only Author and Title

Hruz, T., Laule, O., Szabo, G., Wessendorp, F., Bleuler, S., Oertle, L., Widmayer, P., Gruissem, W. and Zimmermann, P. (2008). Genevestigator v3: a reference expression database for the meta-analysis of transcriptomes. Advances in bioinformatics.
Pubmed: Author and Title
Google Scholar: Author Only Title Only Author and Title

Itoh, H., Matsuoka, M., and Steber, C.M. (2003). A role for the ubiquitin-26S-proteasome pathway in gibberellin signaling. Trends Plant Sci 8, 492–497.
Pubmed: Author and Title
Google Scholar: Author Only Title Only Author and Title

Itoh, H., Sasaki, A., Ueguchi-Tanaka, M., Ishiyama, K., Kobayashi, M., Hasegawa, Y., Minami, E., Ashikari, M., and Matsuoka, M. (2005). Dissection of the phosphorylation of rice DELLA protein, SLENDER RICE1. Plant Cell Physiol. 46, 1392–1399.
Pubmed: Author and Title
Google Scholar: Author Only Title Only Author and Title

Li, K., Yu, R., Fan, L.M., Wei, N., Chen, H. and Deng, X.W. (2016). DELLA-mediated PIF degradation contributes to coordination of light and gibberellin signalling in Arabidopsis. Nature communications, 7, p.11868.
Pubmed: Author and Title
Google Scholar: Author Only Title Only Author and Title

Li, S.-J., and Hochstrasser, M. (2003). The Ulp1 SUMO isopeptidase: distinct domains required for viability, nuclear envelope localization, and substrate specificity. 160, 1069.

Pubmed: Author and Title
Google Scholar: Author Only Title Only Author and Title

Luís, I.M., Alexandre, B.M., Oliveira, M.M., and Abreu, I.A. (2016). Selection of an Appropriate Protein Extraction Method to Study the Phosphoproteome of Maize Photosynthetic Tissue. Plos One 11, e0164387.
Pubmed: Author and Title
Google Scholar: Author Only Title Only Author and Title

Mann, D.G.J., LaFayette, P.R., Abercrombie, L.L., King, Z.R., Mazarei, M., Halter, M.C., Poovaiah, C.R., Baxter, H., Shen, H., Dixon, R.A., et al. (2011). Gateway-compatible vectors for high-throughput gene functional analysis in switchgrass (Panicum virgatum L.) and other monocot species. - PubMed - NCBI. Plant Biotechnol. J. 10, 226–236.
Pubmed: Author and Title
Google Scholar: Author Only Title Only Author and Title

Marín-de la Rosa, N., Pfeiffer, A., Hill, K., Locascio, A., Bhalerao, R.P., Miskolczi, P., Grønlund, A.L., Wanchoo-Kohli, A., Thomas, S.G., Bennett, M.J. and Lohmann, J.U. (2015). Genome wide binding site analysis reveals transcriptional coactivation of cytokinin-responsive genes by DELLA proteins. PLoS genetics, 11(7), p.e1005337.
Pubmed: Author and Title
Google Scholar: Author Only Title Only Author and Title

Miura, K., Jin, J.B., and Hasegawa, P.M. (2007). Sumoylation, a post-translational regulatory process in plants. Current Opinion in Plant Biology 10, 495–502.
Pubmed: Author and Title
Google Scholar: Author Only Title Only Author and Title

Moraes, G.P., Benitez, L.C., do Amaral, M.N., Vighi, I.L., Auler, P.A., da Maia, L.C., Bianchi, V.J., and Braga, E.J.B. (2015). Evaluation of reference genes for RT-qPCR studies in the leaves of rice seedlings under salt stress. Genet. Mol. Res. 14, 2384–2398.
Pubmed: Author and Title
Google Scholar: Author Only Title Only Author and Title

Munns, R., and Tester, M. (2008). Mechanisms of salinity tolerance. Annu. Rev. Plant Biol. 59, 651–681.
Pubmed: Author and Title
Google Scholar: Author Only Title Only Author and Title

Negrão, S., Courtois, B., Ahmadi, N., Abreu, I., Saibo, N., and Oliveira, M.M. (2011). Recent Updates on Salinity Stress in Rice: From Physiological to Molecular Responses. Critical Reviews in Plant Sciences 30, 329–377.
Pubmed: Author and Title
Google Scholar: Author Only Title Only Author and Title

Nelis, S., Conti, L., Zhang, C., and Sadanandom, A. (2015). A functional Small Ubiquitin-like Modifier (SUMO) interacting motif (SIM) in the gibberellin hormone receptor GID1 is conserved in cereal crops and disrupting this motif does not abolish hormone dependency of the DELLA-GID1 interaction. Plant Signaling & Behavior 10, e987528.
Pubmed: Author and Title
Google Scholar: Author Only Title Only Author and Title

Otomo, K., Kenmoku, H., Oikawa, H., König, W.A., Toshima, H., Mitsuhashi, W., Yamane, H., Sassa, T., and Toyomasu, T. (2004). Biological functions of ent- and syn-copalyl diphosphate synthases in rice: key enzymes for the branch point of gibberellin and phytoalexin biosynthesis. Plant J. 39, 886–893.
Pubmed: Author and Title
Google Scholar: Author Only Title Only Author and Title

Pabuayon, I.M., Yamamoto, N., Trinidad, J.L., Longkumer, T., Raorane, M.L., and Kohli, A. (2016). Reference genes for accurate gene expression analyses across different tissues, developmental stages and genotypes in rice for drought tolerance. Rice 9, 32.
Pubmed: Author and Title
Google Scholar: Author Only Title Only Author and Title

Rosa, M.T.G., Almeida, D.M., Pires, I.S., da Rosa Farias, D., Martins, A.G., da Maia, L.C., de Oliveira, A.C., Saibo, N.J.M., Oliveira, M.M., and Abreu, I.A. (2018). Insights into the transcriptional and post-transcriptional regulation of the rice SUMOylation machinery and into the role of two rice SUMO proteases. BMC Plant Biol 18, 349.
Pubmed: Author and Title
Google Scholar: Author Only Title Only Author and Title

Sakai, H., Lee, S.S., Tanaka, T., Numa, H., Kim, J., Kawahara, Y., Wakimoto, H., Yang, C.-C., Iwamoto, M., Abe, T., et al. (2013). Rice Annotation Project Database (RAP-DB): an integrative and interactive database for rice genomics. - PubMed - NCBI. Plant Cell Physiol. 54, e6–e6.
Pubmed: Author and Title
Google Scholar: Author Only Title Only Author and Title

Sakamoto, T., Sakakibara, H., Kojima, M., Yamamoto, Y., Nagasaki, H., Inukai, Y., Sato, Y., and Matsuoka, M. (2006). Ectopic Expression of KNOTTED1-Like Homeobox Protein Induces Expression of Cytokinin Biosynthesis Genes in Rice. Plant Physiology 142, 54–62.
Pubmed: Author and Title
Google Scholar: Author Only Title Only Author and Title

Sarhadi, E., Bazargani, M.M., Sajise, A.G., Abdolahi, S., Vispo, N.A., Arceta, M., Nejad, G.M., Singh, R.K., and Salekdeh, G.H. (2012). Proteomic analysis of rice anthers under salt stress. Plant Physiology and Biochemistry 58, 280–287.

Pubmed: Author and Title
Google Scholar: Author Only Title Only Author and Title

Srivastava, A.K., Zhang, C., and Sadanandom, A. (2016a). Rice OVERLY TOLERANT TO SALT 1 (OTS1) SUMO protease is a positive regulator of seed germination and root development. Plant Signaling & Behavior 11, e1173301.
Pubmed: Author and Title
Google Scholar: Author Only Title Only Author and Title

Srivastava, A.K., Zhang, C., Caine, R.S., Gray, J., and Sadanandom, A. (2017). Rice SUMO protease Overly Tolerant to Salt 1 targets the transcription factor, OsbZIP23 to promote drought tolerance in rice. The Plant Journal 92, 1031–1043.
Pubmed: Author and Title
Google Scholar: Author Only Title Only Author and Title

Srivastava, A.K., Zhang, C., Yates, G., Bailey, M., brown, A., and Sadanandom, A. (2016b). SUMO is a critical regulator of salt stress responses in rice. Plant Physiology 170, pp.01530.2015–pp.01530.2391.
Pubmed: Author and Title
Google Scholar: Author Only Title Only Author and Title

Su, G., Morris, J.H., Demchak, B., and Bader, G.D. (2014). Biological network exploration with Cytoscape 3. - PubMed - NCBI. Current Protocols in Bioinformatics 47, 8.13.1–8.13.24.
Pubmed: Author and Title
Google Scholar: Author Only Title Only Author and Title

Ueguchi-Tanaka, M., Hirano, K., Hasegawa, Y., Kitano, H., and Matsuoka, M. (2008). Release of the repressive activity of rice DELLA protein SLR1 by gibberellin does not require SLR1 degradation in the gid2 mutant. Plant Cell 20, 2437–2446.
Pubmed: Author and Title
Google Scholar: Author Only Title Only Author and Title

Ulrich, H.D. (2008). The fast-growing business of SUMO chains. Mol. Cell 32, 301–305.
Pubmed: Author and Title
Google Scholar: Author Only Title Only Author and Title

Van De Velde, K., Ruelens, P., Geuten, K., Rohde, A., and Van Der Straeten, D. (2017). Exploiting DELLA Signaling in Cereals. Trends Plant Sci.
Pubmed: Author and Title
Google Scholar: Author Only Title Only Author and Title

Vanstraelen, M., and Benková, E. (2012). Hormonal interactions in the regulation of plant development. Annu. Rev. Cell Dev. Biol. 28, 463–487.
Pubmed: Author and Title
Google Scholar: Author Only Title Only Author and Title

Werner, A., Moutty, M.-C., Möller, U., and Melchior, F. (2009). Performing in vitro sumoylation reactions using recombinant enzymes. Methods Mol. Biol. 497, 187–199.
Pubmed: Author and Title
Google Scholar: Author Only Title Only Author and Title

Xue, Y., Zhou, F., Fu, C., Xu, Y., and Yao, X. (2006). SUMOsp: a web server for sumoylation site prediction. Nucleic Acids Research 34, W254–W257.
Pubmed: Author and Title
Google Scholar: Author Only Title Only Author and Title

Yang, C., Ma, Y., and Li, J. (2016). The rice YABBY4 gene regulates plant growth and development through modulating the gibberellin pathway. J. Exp. Bot. 67, erw319–erw5556.
Pubmed: Author and Title
Google Scholar: Author Only Title Only Author and Title

Yano, K., Morinaka, Y., Wang, F., Huang, P., Takehara, S., Hirai, T., Ito, A., Koketsu, E., Kawamura, M., Kotake, K. and Yoshida, S., 2019. GWAS with principal component analysis identifies a gene comprehensively controlling rice architecture. Proceedings of the National Academy of Sciences, 116(42), pp.21262-21267.
Pubmed: Author and Title
Google Scholar: Author Only Title Only Author and Title

Yates, G., Srivastava, A.K., and Sadanandom, A. (2016). SUMO proteases: uncovering the roles of deSUMOylation in plants. J. Exp. Bot. 67, 2541–2548.
Pubmed: Author and Title
Google Scholar: Author Only Title Only Author and Title

Zentella, R., Hu, J., Hsieh, W.P., Matsumoto, P.A., Dawdy, A., Barnhill, B., Oldenhof, H., Hartweck, L.M., Maitra, S., Thomas, S.G. and Cockrell, S. (2016). O-GlcNAcylation of master growth repressor DELLA by SECRET AGENT modulates multiple signaling pathways in Arabidopsis. Genes & development, 30(2), pp.164-176.
Pubmed: Author and Title
Google Scholar: Author Only Title Only Author and Title

Zentella, R., Sui, N., Barnhill, B., Hsieh, W.-P., Hu, J., Shabanowitz, J., Boyce, M., Olszewski, N.E., Zhou, P., Hunt, D.F., et al. (2017). The

Arabidopsis O-fucosyltransferase SPINDLY activates nuclear growth repressor DELLA. Nat. Chem. Biol. 21, 985–485.

Pubmed: Author and Title
Google Scholar: Author Only Title Only Author and Title